Design and Implementation of Electrode Holder and Electrode Consumption System for Educational Welding Simulator for SMAW

Design and Implementation of Electrode Holder and Electrode Consumption System for Educational Welding Simulator for SMAW

M Yasser[1] and A Badawy`[1]

[1]Faculty of Engineering, Mechatronics Department, MSA University, 6th October, Egypt
E-mail: mohammed.yasser2@msa.edu.eg

Abstract. Shielded metal arc welding is one of the common welding operations in various industries. SMAW requires a lot of training. And for new trainees, sparks, high voltage and temperature could impose a potential risk. Moreover, welding training drains a lot of financial resources. The introduction of welding simulators in the initial training phases solves this problem. It provides safe environment and simulates the welding environment. Thus, electrode consumption simulation is required to mimic the real welding environment. Furthermore, simulating electrode consumption with a physical system obviate the need for real electrode. For evaluating the trainee skills, the welding parameters such as holder orientations, arc length and travel speed are measured. These parameters are then used for trainees' assessment as they affect the welding quality. The proposed solution uses stepper motor, rack and pinion to simulate electrode consumption. The orientation of the electrode holder and the travel speed is tracked by an inertia measurement unit. An extended Kalman filter is designed for orientation estimation. The arc length is measured using time of flight sensor. Two filtration methods for time-of-flight sensor are implemented and compared. The accuracy of orientation and arc length measurements is found to be reliable and suitable for the system.

1. Introduction

Welding is a vital process in various industries, such as car manufacturing, airplane, ships and nuclear plants. As welding is a joining process using filer material and heat or pressure. In shielded metal arc welding (SMAW) a consumable electrode is used as a filer material and the heat is generated from an electric arc. The electric arc can produce a temperature up to 5000℃ [1]. Thus, welders must take safety precautions to avoid electric and heat hazards. Moreover, the exposure to welding fumes and gases is related to various diseases [2]. This harsh environment can represent a challenge for beginner welders specially in young age. Another downside of traditional welding training is consumable materials as they raise the training cost and produce waste. By using a virtual environment without any hazards or material consumption, welding simulators can be an effective training and testing alternative to traditional training. Welding simulators usually include hardware in the shape of electrode holder or welding torch. The purpose of the hardware is to track the motion of the torch. From the orientation and speed the welding quality and the welder skills can be evaluated. Moreover, these parameters can be used to visualize the virtual welding process. In the current century various welding simulators are

designed. Despite the type of welding process, the same principle is applied for motion tracking. The approaches that have been used for tracking the torch movement can be divided into three methods: tracking using inertia measurement unit (IMU), using cameras and optical sensors, and combining both cameras and IMU [3] [4] [5] [6]. IMUs are implemented in various systems for motion tracking as they usually consist of three sensors: accelerometer, gyroscope, and magnetometer. The orientation is estimated using the readings of the three sensors [7]. While the speed is estimated using acceleration readings. On the other hand, tracking using cameras can be more sophisticated as it requires designing the mounting surface for the cameras and tracking markers. As well as it requires more computational power than using IMU [8]. Also, the development of micro-electromechanical (MEMS) IMUs gives upper hand to IMUs over tracking using camera. As IMUs can be a cost-effective option. In SMAW arc length affects the welding quality and must be kept between 1.5 to 4 mm [9]. One of the approaches used is measuring the arc length using linear variable differential transformer (LVDT) [4]. However, LVDT is an expensive option and can be replaced with cheaper proximity, time of flight (ToF), or IR sensor. To accurately simulate the real welding environment, SMAW simulator mimic the consuming rate. In BasVW 1.1 SMAW simulator the electrode consumption system is implemented using direct current (DC) motor, gearbox and lead screw [4].

2. Theoretical Model

The electrode holder is supposed to simulate actual holder used in real welding in shape and size. Moreover, the consumption system and sensors will be contained inside the holder. Thus, component selection especially focuses on the size. The proposed design of the holder is shown in figure 1. Electrode consumption can be simplified as motor coupled with a rotational to linear motion mechanism. The proposed design uses a rack and pinion mechanism.

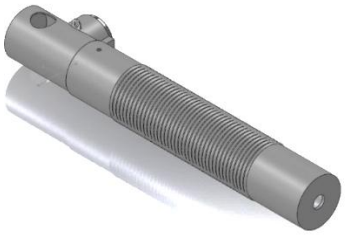

Figure 1. Electrode Holder Design

There are no loads exerted on the rack as it does not transport any mass. The rack weight is small and could be neglected. For the pinion, the torque applied on it is the motor torque. Since the system has low load, small size and require precision movement gear module of 1 is selected. To calculate the minimum number of teeth to avoid undercutting could be calculated using equation (1) where ϕ is the pressure angle equals 20 degrees.

$$N_{min} = \frac{2}{\sin^2(\phi)} \quad (1)$$

The pitch circular diameter D_{pc}could be obtained by multiplying the number of teeth (Z) with the gear module (M). The distance travelled by the rack per revolution could be obtained from equation (2). The rack pitch calculated from equation (3).

$$Distance = \pi \times D_{pc} \quad (2)$$

$$Pitch = \frac{\pi \times D_{pc}}{Z} \quad (3)$$

Since the rack is supposed to simulate the electrode in dimension the rod containing rack length would be 34 cm and the actual rack length would be 31 cm. Therefore, the required number of teeth from rack obtained using equation (4). The pinion is connected to a stepper motor. Using micro stepping the motor can move the rack with the required speed to simulate the electrode consuming rate. The consuming rate varies according to electrode diameter and type. The proposed system will simulate a 3.25 mm diameter electrode E6010 with consumption rate around 3.7 mm/s [9]

$$Z_{rack} = \frac{Rack\ Length}{Pitch} \tag{4}$$

The required motor speed is the pinion speed which is calculated using equation (5). The required number of steps could be calculated using equation (6). Where the number of steps per revolution is calculated using equation (7). If micro stepping is used, the value of steps per revolution is calculated by multiplying the factor of micro stepping with steps per second value.

$$\omega_{pinion}\ (RPM) = \frac{v_{rack} \times 60}{\pi D_p} \tag{5}$$

$$steps\ per\ second = \frac{steps\ per\ rev \times \omega_{pinion}}{60} \tag{6}$$

$$steps\ per\ rev = \frac{360}{step\ angle} \tag{7}$$

Since IMU sensors are very noisy environment. And depending on the raw data measurement can lead to large estimation error. Various filtering techniques are used with IMU sensors to improve the quality of reading and eliminate the noise effect. The IMU used herein is BNO055. BNO055 integrates 3 axis gyroscope, 3 axis magnetometer and 3 axis accelerometers. The sensor uses I2C communication protocol. Also, the sensor offers output orientation as Euler angle, quaternion or vector form. For applying EKF, first the model of gyroscope, accelerometer and magnetometer should be obtained as shown in equation (8), (9) and (10) respectively [10].

$$H_g = \omega_{x,y,z} + v_g + O_g \tag{8}$$

$$H_a = R^{bn}(a - g) + v_g + O_a \tag{9}$$

$$H_m = R^{bn} \times m + v_g + O_m \tag{10}$$

Where $\omega_{x,y,z}$ is the angular velocity and v_g is a noise assumed to be white Gaussian noise. R^{bn} is the rotation matrix from body frame to navigation frame, a is the linear acceleration, g is the gravity and m is the magnetic field. Then a state vector is to be defined as in equation (11) [11]. The r is a vector donated for the orientation (roll, pitch, and yaw), the ω is the angular velocity. The acceleration obtained from accelerometer is donated as a and the magnetic field readings is m. Those states are not containing the offsets off the sensors. The offsets for gyroscope, accelerometer and magnetometer are represented as O_g, O_a and O_m respectively.

$$X = [r^T \quad \omega^T \quad a^T \quad m^T \quad O_g^T \quad O_a^T \quad O_m^T]^T \tag{11}$$

The initial estimation of the orientation is done by assuming that the sensor is stationary. Thus, the accelerometer is only affected by gravity. And hence no motion at the start of the accelerometer readings is the gravity vector. The gravity vector g has three components for each direction (x, y and z). The magnitude of the gravity vector equals 9.8 m/s^2. The pitch angle is shown in equation (12) obtained by the projection of the gravity vector in yz plane. The roll angle is shown in equation (13). Thus, a rotation matrix describes the transformation between the IMU frame, and the earth frame could be obtained as shown in equation (14) [11] [12].

$$\theta = atan2(-a_x\ , \sqrt{a_y^2 + a_z^2}\ ) \tag{12}$$

$$\varphi = atan2(a_y\ , a_z\ ) \tag{13}$$

$$R = \begin{bmatrix} \cos(\theta) & \sin(\theta) \times \sin(\varphi) & \sin(\theta) \times \cos(\varphi) \\ 0 & \cos(\varphi) & -\sin(\varphi) \\ -\sin(\theta) & \sin(\varphi) \times \cos(\theta) & \cos(\theta) \times \cos(\varphi) \end{bmatrix} \tag{14}$$

The rotation matrix and the magnetometer readings are used to estimate the yaw angle. First, the magnetic field vector represents the magnetometer readings in x, y and z multiplied by the rotation matrix R to transform it from the IMU frame to the earth frame. Then the yaw angle is calculated as shown in equation (15) [12] by using the x and y components of the transformed magnetic field vector.

$$\gamma = arctan(-(R \times m)_y\ , (R \times m)_x) \tag{15}$$

The EKF algorithm contains two steps, the first one is prediction and the second is the correction. For the prediction step, y_t is the function maps the measured states x_t to the inputs u_t which considered the

output of the filter. As shown in equation (16) [11] the covariance matrix C is obtained, which represents the uncertainty in estimated states. Where the dynamic covariance matrix D is calculated by partially differentiating the y_t with respect to the current states x_t. The J matrix is the derivative of the y_t with respect to the system input u_t, and Q is the noise. In the correction step, the measure sensitivity matrix S is the partial derivative of measurement prediction y at time t with respect to system states X.

$$C_{t+1} = D_t\, C_t\, D_t^T + J_t Q\, J_t^T \tag{16}$$

The estimated states x at the time t is shown in equation (17), where K is the Kalman gain. The IM is innovation matrix which represents the difference between the estimated and the actual output is calculated as shown in equation (18). The innovation i which represents the difference as the IM is shown in equation (19). Then the covariance matrix is updated as in equation (20). The gain is calculated is shown in equation (21) [11].

$$x_t = x_{t-1} + K_t \times i_t \tag{17}$$
$$IM = S_t C_{t-1} S_t^T + R_t \tag{18}$$
$$i = (y_t)_{actual} - (y_t)_{estimated} \tag{19}$$
$$C_t = C_{t-1} - K_t IM_t K_t^T \tag{20}$$
$$K_t = C_{t-1} S_t IM_t^{-1} \tag{21}$$

At each iteration, the states vector is updated, each sensor measurement estimation and offsets are updated. The angular and velocity and gyroscope's offset update are shown in equation (22) and (23). The acceleration and accelerometer offset is shown in equation (24) and (25) [11].

$$\omega_{t+1} = H_{g,t} - O_{g,t} - v_g \tag{22}$$
$$O_{g,t+1} = eO_t + v_g \tag{23}$$
$$a_{t+1} = H_{a,t} + R_t\,(g - O_{a,t}) - v_g \tag{24}$$
$$O_{a,t+1} = eO_{a,t} + v_g \tag{25}$$

The magnetic field readings and magnetometer offset equations (26) and (27). For updating the states vector the algorithm used a quaternion for the rotation obtained in the initialization state by converting the rotation matrix to quaternion. The quaternion representing orientation then updated as shown in equation (28). Also, the rotation at the next step is calculated as in equation (29), where T is the sampling time set to 50 samples per second. Then state vector is updated in equation (30) [11].

$$m_{t+1} = H_{m,t} + R_t\, O_{m,t} - v_g \tag{26}$$
$$O_{m,t+1} = eO_{m,t} + v_g \tag{27}$$
$$q_t = \exp\left(\frac{X_t}{2}\right) q_{t-1} \tag{28}$$
$$q_{t+1} = q_t \exp(T\frac{\omega_t}{2}) \tag{29}$$
$$X_{t+1} = 2\log(\exp\left(\frac{X_t}{2}\right) q_t \exp\left(T\frac{H_{g,t} - O_{g,t} - v_g}{2}\right) q_{t+1}) \tag{30}$$

Arc length measurement is an important function for ensuring welding quality. The arc length ranges in few millimeters thus the sensor should be able to sense 1 mm distance change. However, Vl53l0X output readings subjected to noise affecting its quality. Moreover, the sensor will be mounted on the electrode tip, thus the inclination of the electrode in z axis should be considered to obtain accurate distance between the electrode tip and the workpiece. The arc length measurement system description is shown in Figure 2. The input data from the sensor passes through the filter to eliminate the noise for accurate distance measurement. Then if the arc length is within the acceptable range, then welding occurs. If not, the welding process stops until the arc length value becomes within the range.

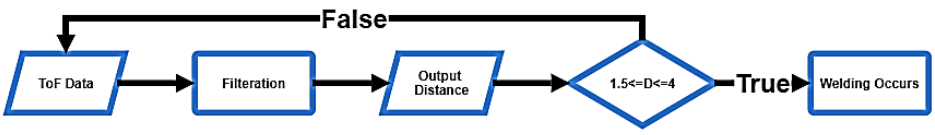

Figure 2. Arc Length Measurement System Flowchart

A median filter is used to filter the noise and estimate distance. Median filter is a nonlinear filtering technology that is widely used in a variety of industries due to their ability to remove noise while preserving edges. It is particularly effective at removing salt-and-pepper noise from signals or images. The flow of the filter construction could be defined in the following steps [13]:

- Input Data
- Calculate the median of the data
- Output filtered data

Another experiment conducted using wavelet filtering. The wavelet filter is a signal processing technique that transforms data into another domain for analysis and filtering. It incorporates wavelet transformations, which decompose signals into frequency components that can then be selectively altered, such as noise removal and compression. The flow of the filter could be defined in the following steps [13]:

- Decomposing: approximation Coefficients are low-frequency, smooth fluctuations that carry the main signal. And detail coefficients are high-frequency changes that frequently contain noise. This is accomplished using a wavelet function
- Thresholding: It involves adjusting or removing detail coefficients to reduce noise.
- Inverse Wavelet Transform: Reconstruct the signal using updated coefficients.

The implementation of the feedback system in the electrode holder will be done using a controller and motor. The system design is shown in Figure 3. A pulse width modulation (PWM) pin is connected to the gate pin for the MOSFET. When the signal is high the MOSFET turns on, running the motor. As the signal is low the MOSFET turns off which stops the motor. The pull-down resistance pulls the MOSFET gate to ground when low signal is applied through PWM pin. When the signal drops to low, the flywheel diode eliminates voltage spikes. The capacitor eliminates high frequency noise caused by MOSFET switching on and off. When the measured values of orientation from the IMU exceed these values, the feedback starts until the user corrects its orientation. As the same with the welding angles any derivation around the optimum speed value obtained from the IMU will start the vibration until the user reach the optimum speed. Furthermore, if the measured value from ToF is outside the range the vibration starts.

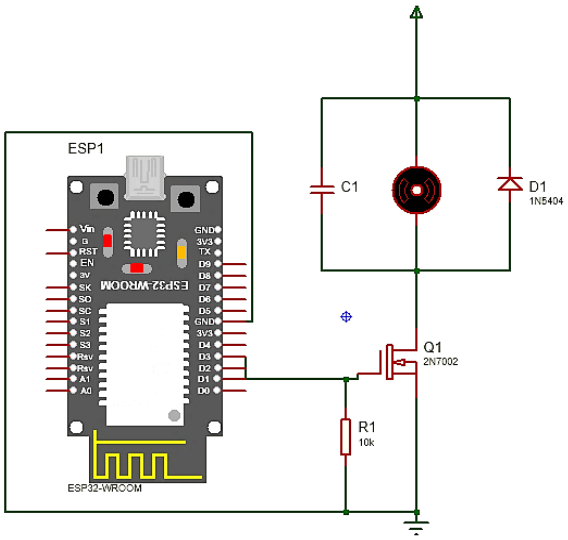

Figure 3. Feedback system Design

3. Results

The final implementation of electrode holder and consumption system are shown in figure 4. Where the rack represents the electrode. The rack and pinion dimensions are shown in table 1. The EKF for BNO055 IMU sensor is deployed on ESP32 microcontroller. The measured pitch, roll and yaw angles from the sensor and actual ones are then compared, Figure 5. The error in the measured angle is less

than 1 degree. To test if the orientation measurement is suffering from drifts the gun is held in a fixed position with roll angle 60 degrees. Then the IMU readings are recorded and compared to the actual orientation as shown in figure 6. As shown from the figure the drift error is around zero for around two minutes.

Figure 4. Electrode Holder Implementation

Table 1. Rack and Pinion Dimensions

Parameter	Value
Gear Type	Spur
Module	1
Minimum Number of Teeth	17
Number of Pinion Teeth	17
Circular Diameter (mm)	17
Distance Traveled by Rack per Revolution (mm/rev)	53
Rack Pitch (mm)	3
Number of Rack Teeth	98

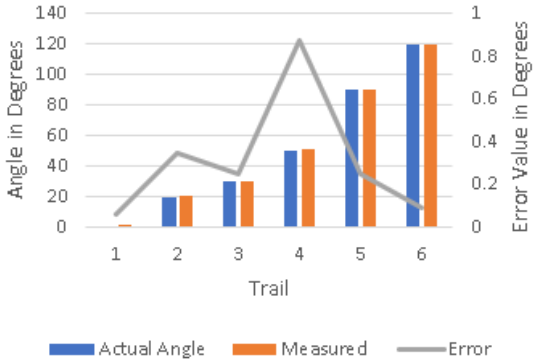

(a) comparison between measured pitch angle and actual angle

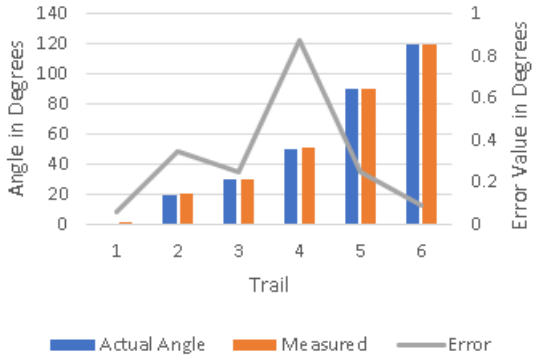

(b) comparison between measured yaw angle and actual angle

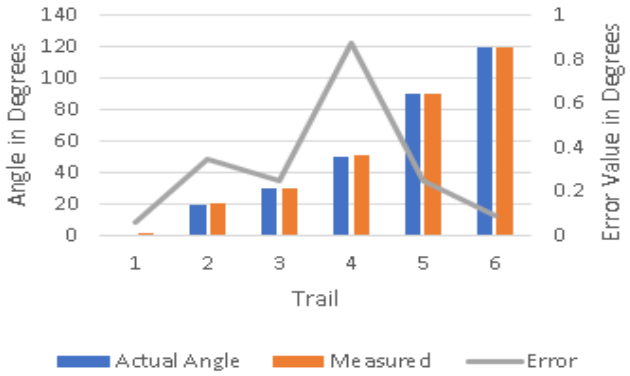

(c) comparison between measured pitch angle and actual angle

Figure 5. Comparison between actual angles and measured angles from BNO055

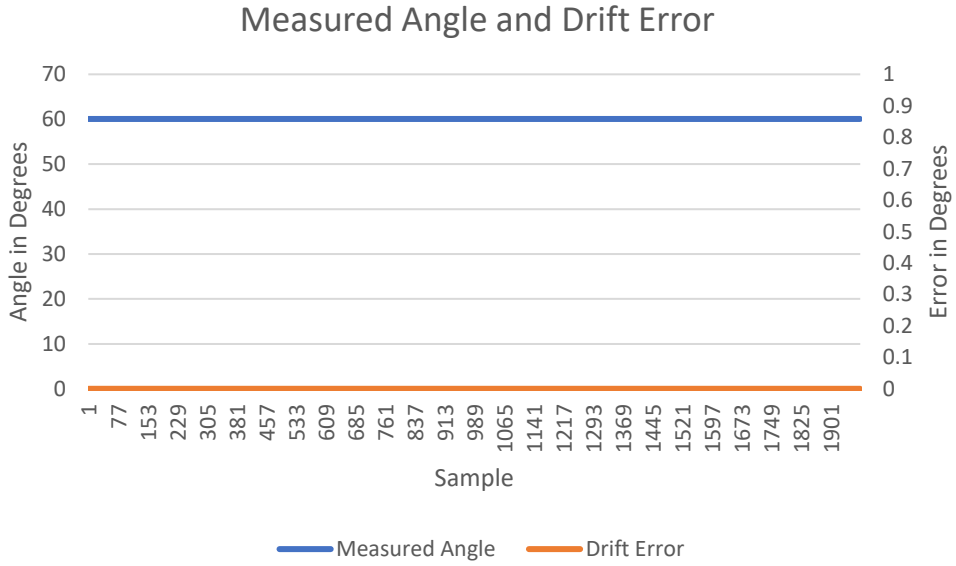

Figure 6. Measured Roll Angle and Drift Error Measured by the Electrode Holder

Travel Speed or the speed of the electrode holder is a critical parameter in welding quality. The speed should be maintained constant, thus the acceleration can indicates changes in the travel speed. A recorded data sample from the linear acceleration is shown in figure 7 measured during testing. These values indicates the user trails to maintain zero acceleration to achieve constant speed. Figure 8 illustrate the orientation error in each angle, which is the difference between the optimum angle and measured one.

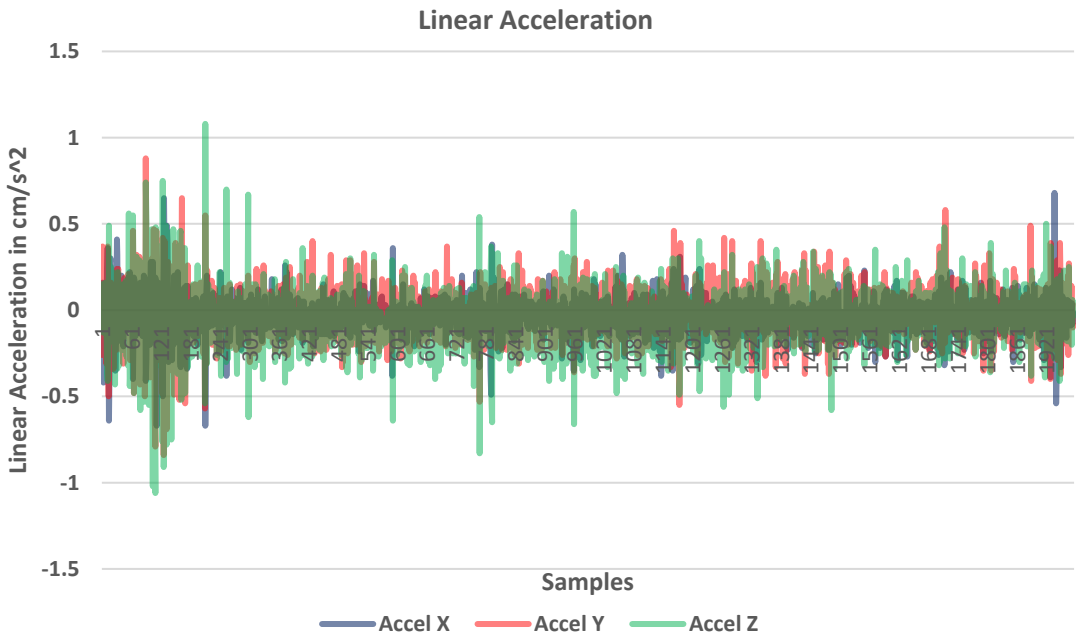

Figure 7. Acceleration Profile of the Electrode Holder during Testing

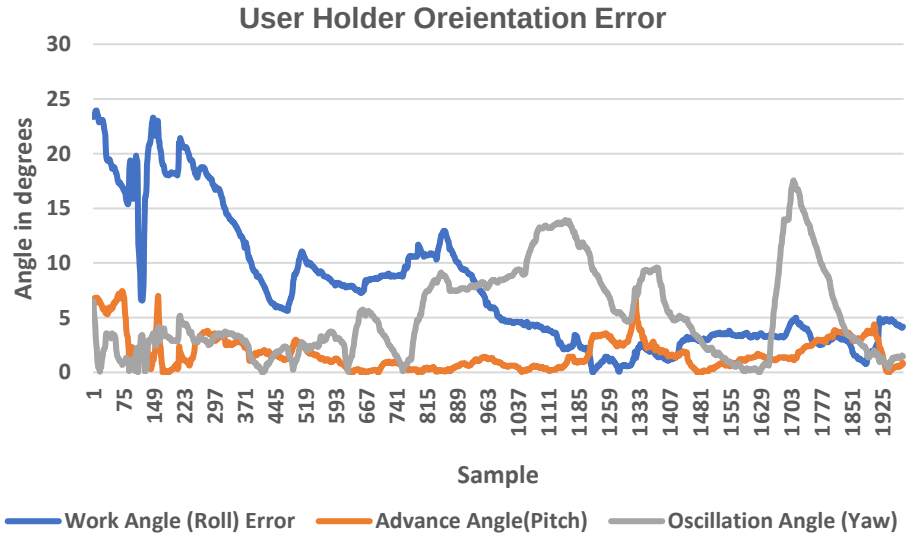

Figure 8. User Electrode Holder Orientation Error

For validating the arc length measurement system, another experiment is conducted. The ToF sensor is mounted on the rack tip. The electrode holder is held, thus the arc length would be 35 mm. The readings from the sensor and the error are shown in Figure 9. Where the reading is taking 6 times for the same

distance. This experiment is done for comparing median filter and wavelet filter. The wavelet filter is selected, hence it has higher precision than the median filter.

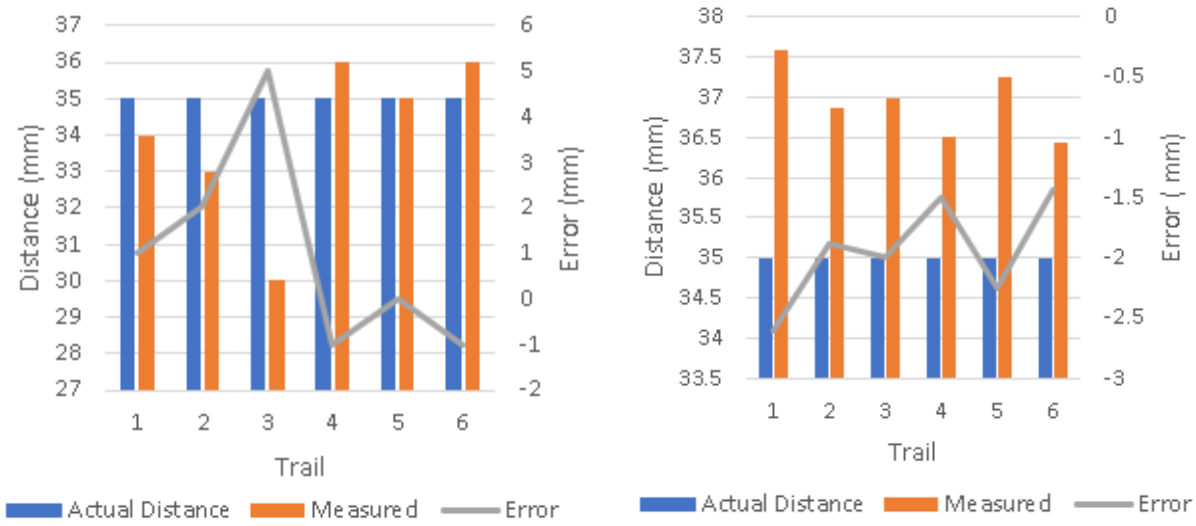

(a) Distance estimation from ToF sensor by applying a median filter.

(b) Distance estimation from ToF sensor by applying wavelet-based filter.

Figure 9. Comparison between actual distance and measured distance after filtration

Welding quality is affected by the electrode orientation and arc length. Furthermore these parameters used to calculate the weld bead size for accurate welding assessment. Thus the accuracy in measuring these parameter lead to more accurate assessment. Moreover the feedback provided by the vibration motor can assets the user and indicates when the orientation of the electrode exceeds the optimum value. As well as with the arc length readings from the Tof sensor when the value exceeds its optimum value the vibration indicates this event. The implemented system can help beginner welders to learn and improve their skills in safe environment. With the capability of accurately detecting orientation and measuring the arc length. While maintaining the no material consumption as the training process does not require electrode or test pieces to weld. Also, no high temperature or electric hazard exist in the training process for safe environment to encourage beginner welders to practice at any places without any safety precautions needed.

4. Conclusions

Some of the most vital elements of a welding simulation system have been successfully built, put into practice, and tested in this paper. The electrode holder and consumption system were made to accurately replicate actual welding conditions. To improve user interaction with realistic force feedback was designed. The BNO055 sensor and extended Kalman filter were used in the development of the orientation measurement system, which have an inaccuracy of less than 1 degree. The IMU data is tested for draft errors and had proven its reliability for the measurement system. As the drift error is nearly zero. This level of accuracy allows for accurate tracking of the welder's movements, which enhances the simulation's realism and user assessment. To efficiently monitor welding conditions, an arc measurement system was also created and tested. Wavelet based filter and median filter are compared. Wavelet filter error in distance estimation is around ±2 mm. While median filter error ranges between 1 to 5 mm. Moreover, the wavelet filter is found to be higher in precision compared to the median filter. For wavelet filter the error in the readings could be considered as a fixed bias that will be

subtracted from the reading. To conclude, the overall system can be used in training new welders and asset there performance with high accuracy. Since, the system simulates the SMAW electrode holder and track the holder motion with a compact small size system. The training can be conducted at any place and is not restricted to workshops.

References

[1] H Liu and Y HU 2022 Welding in *Encyclopedia of Materials: Metals and Alloys*, Elsevier, pp. 39-65.

[2] R Chakradhar, J O Moody, K Jenab and S Moslehpour 2022 Improving the quality of welding training with the help of mixed reality along with the cost reduction and enhancing safety, *Management Science Letters,* vol. 12, no. 4, pp. 321-330.

[3] T L Chambers, D Reiners, A Aglawe and S A White 2012 Real-time simulation for a virtual reality-based MIG welding training system, *Virtual Reality,* vol. 16, no. 1, pp. 45-55, March 2012.

[4] R. Khazal 2013 Design and Construction of Virtual Welding Training System for the Shielded Metal Arc Welding (SMAW)

[5] K Shankhwar, T-J Chuang, Y-Y Tsai and S Smith 2022 A visuo-haptic extended reality–based training system for hands-on manual metal arc welding training, *The International Journal of Advanced Manufacturing Technology,* vol. 121, pp. 249-265.

[6] B Xie, Q Zhou and L Yu 2015 A real-time welding training system based on virtual reality, in *2015 IEEE Virtual Reality (VR)*, Arles, France.

[7] L Chen, S. Wang, H Hu, D Gu and I Dukes, 2008 Chapter 17 - Voice-directed autonomous navigation of a smart-wheelchair, in *Smart Wheelchairs and Brain-Computer Interfaces*, Elsevier, pp. 405-424.

[8] J Li, M Slembrouck, F Deboeverie, A M Bernardos, J A Besada, P Veelaert, H Aghajan, J R Casar and W Philips 2016 Handheld pose tracking using vision-inertial sensors with occlusion handling," *Journal of Electronic Imaging,* vol. 25, no. 4.

[9] U Soy, O. Iyibilgin, F Findik, C Oz and Y Kiyan 2011 Determination of welding parameters for shielded metal arc welding, *Scientific Research and Essays,* vol. 6, no. 15, pp. 3153-3160.

[10] T Zheng, A Xu, X Xu and M Liu 2023 Modeling and Compensation of Inertial Sensor Errors in Measurement Systems, *Electronics,* vol. 12, no. 11.

[11] S B Farahan, J J M Machado, F G d Almeida and J M R S Tavares 2022 9-DOF IMU-Based Attitude and Heading Estimation Using an Extended Kalman Filter with Bias Consideration, *Sensors,* vol. 22, No. 9.

[12] Z Xu, J Tian, T Chao, M Yang and K Fang 2023 An Adaptive Extended Kalman Filter for Attitude Estimation Using Low-Cost IMU from Motor Vibration Disturbance, Tianjin, China, 20.

[13] J D Broesch 2008 Digital Filters, in *Digital Signal Processing*.